ISSN 0015-4628, Fluid Dynamics, 2009, Vol. 44, No. 1, pp. 141–157. © Pleiades Publishing, Ltd., 2009.
Original Russian Text © A.N. Volkov, 2009, published in Izvestiya Rossiiskoi Akademii Nauk, Mekhanika Zhidkosti i Gaza, 2009, Vol. 44, No. 1, pp. 167–187.

Aerodynamic Coefficients of a Spinning Sphere in a Rarefied-Gas Flow

A. N. Volkov

Received December 17, 2007

Abstract—A three-dimensional rarefied-gas flow past a spinning sphere in the transitional and near-continuum flow regimes is studied numerically. The rarefaction and compressibility effects on the lateral (Magnus) force and the aerodynamic torque exerted on the sphere are investigated for the first time. The coefficients of the drag force, the Magnus force, and the aerodynamic torque are found for Mach numbers ranging from 0.1 to 2 and Knudsen numbers ranging from 0.05 to 20. In the transitional regime, at a certain Knudsen number depending on the Mach number the Magnus force direction changes. This change is attributable to the increase in the role of normal stresses and the decrease in the contribution of the shear stresses to the Magnus force with decrease in the Knudsen number. A semi-empirical formula for the calculation of the Magnus force coefficient in the transitional flow regime is proposed.

DOI: 10.1134/S0015462809010153

Keywords: spinning sphere, transitional flow regime, drag force coefficient, Magnus force, aerodynamic torque coefficient.

The rotation of a body traveling in a gas or fluid flow may significantly affect the forces and torques exerted on the body by the medium. In particular, an axisymmetric body rotating about a symmetry axis in a fluid flow exhibits the action of a lateral force perpendicular to the translational velocity of the body relative to the medium. The effect of this force on the body trajectory is usually called the Magnus effect and the force is called the Magnus force. It is necessary to take this effect into account in calculating the motion of different spinning bodies, e.g. artillery shells, balls used in sports, and, for instance, dispersed particles in dusty flows. The latter may acquire substantial angular velocities in collisions with other particles or solid surfaces immersed in the flow. In general, the rotation of the body affects all its aerodynamic characteristics.

In this study, we will investigate the aerodynamic coefficients of a spinning sphere. This class of flows is of considerable theoretical and practical importance.

An incompressible flow past a spinning sphere at small Reynolds numbers based on the translational and angular velocities was studied in [1], where the drag and Magnus forces and the aerodynamic torque were obtained using the matched asymptotic expansions method in the form of a two-term expansion in the Reynolds number. The results of [1] are widely used in calculating two-phase flows with spinning particles. These results constituted a basis for subsequent theoretical and experimental studies of the aerodynamics of a spinning sphere. In what follows, we will call the flow regime considered in [1] "the continuum flow regime at small Reynolds numbers".

The experimental and theoretical data for the drag force of a non-spinning sphere have been thoroughly tabulated and represented in the form of semi-empirical formulas [2–9]. In [1] it was shown that at small Reynolds numbers the rotation of the sphere does not affect its drag force coefficient. In [10, 11] a similar result was obtained for the free-molecular flow regime. The effect of rotation on the drag force coefficient at moderate Reynolds numbers was studied in [12], where it was shown that the drag force coefficient of the sphere depends only slightly on the rotation.

In [1], an analytical solution was found for the lateral force acting on a sphere in the continuum regime at small Reynolds numbers. Later, in [12–17], experimental and numerical data were obtained for the lateral

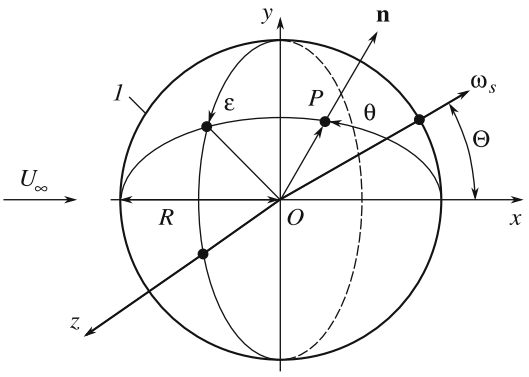

Fig. 1. Cartesian (x, y, z) and spherical r, θ, ε coordinates used for calculating the flow around a spinning sphere and its aerodynamic coefficients: (*1*) sphere.

force in incompressible flows at finite Reynolds numbers. In [1] it was also shown that in the continuum regime at small Reynolds numbers the aerodynamic torque exerted on the spinning sphere is independent of the translational velocity of the sphere relative to the fluid. In [18] the known data for the aerodynamic torque on a sphere rotating in a quiescent incompressible fluid at finite Reynolds numbers based on the angular velocity were generalized and semi-empirical formulas for the torque coefficient were proposed.

In [10] an analytical solution was found for the lateral force acting on the spinning sphere in a free-molecular flow in the case when the vectors of the translational and the angular velocities are perpendicular to each other. In [11] the aerodynamic force and the torque were calculated for an arbitrary axisymmetric body rotating in a free-molecular flow about a symmetry axis. In [10, 11] it was shown that in a rarefied-gas flow in the absence of intermolecular collisions the direction of the lateral force is opposite to that in a continuum flow at small Reynolds numbers. Later, this effect was called the "inverse Magnus effect" [19, 20]. In the present study, we will use the term "Magnus force" in a generalized sense for the lateral component of the aerodynamic force which appears due to the rotation of the body around the symmetry axis, no matter what the flow regime with respect to the Knudsen number. The difference in the Magnus force direction in free-molecular and continuum flows means that in the transitional flow regime the Magnus force depends significantly on the Knudsen number, and, moreover, at a certain value of the Knudsen number this force vanishes. In [21] this critical Knudsen number was found for Mach numbers ranging from 0.1 to 1.

Thus, the aerodynamic coefficients of a spinning sphere are known only for an incompressible flow and a free-molecular flow. The effects of compressibility and rarefaction on the Magnus force and the aerodynamic torque at finite Knudsen numbers remain almost uninvestigated. This study is aimed at calculating the aerodynamic coefficients of a spinning sphere in the transitional and near-continuum flow regimes in which the rarefaction and compressibility effects are predominant.

1. FORMULATION OF THE PROBLEM AND THE MATHEMATICAL MODEL

We will consider the motion of a spinning sphere of radius R in a uniform gas flow. It is assumed that the vectors of the translational $\mathbf{V}_s$ and angular $\boldsymbol{\omega}_s$ velocity of the sphere and the sphere temperature (uniform over the sphere volume) T_s are constant and the flow is steady-state. The flow model is based on the following assumptions:

1) the gas is rarefied and monatomic, its motion can be described using the Boltzmann equation;

2) the intermolecular collisions are described by the rigid-sphere model;

3) the gas molecules interact with the body surface in accordance with the specular-diffusion reflection model;

4) in the uniform free-stream flow, the gas molecule velocity distribution is Maxwellian with the constant concentration n_∞, macroscopic velocity $\mathbf{V}_\infty$, and temperature T_∞.

The use of models which more accurately describe the intermolecular collisions than the rigid-sphere model (for instance, the model based on the Lennard-Jones potential [22] or the VHS molecule model [23]) presents no fundamental difficulties. However, the results obtained in this case are less general because they usually correspond only to a particular species of gas. Preliminary calculations showed that under the conditions considered the details of the intermolecular-collision model only slightly affect the aerodynamic force and the torque. Accordingly, in what follows we present the results obtained for the rigid-sphere model only. The flow is considered in an inertial reference frame fitted to the sphere center O (Fig. 1). In this reference frame, the sphere rotates with the angular velocity $\boldsymbol{\omega}_s$. For calculating the flow, we introduce a Cartesian coordinate system $(x,\ y,\ z)$ with the basis vectors $\mathbf{e}_x$, $\mathbf{e}_y$, and $\mathbf{e}_z$. The x axis is directed along the vector of the gas macroscopic velocity relative to the sphere $\mathbf{U}_\infty = \mathbf{V}_\infty - \mathbf{V}_s$, and the z axis at right angles to the plane of the vectors $\mathbf{U}_\infty$ and $\boldsymbol{\omega}_s$. The location of an arbitrary point P on the sphere surface is specified by the radius-vector $\mathbf{r} = R\mathbf{n}$, where $\mathbf{n}$ is the unit outward normal to the surface of the sphere. For calculating the components of this vector, the angles Θ and ε are used, so that $\mathbf{n} = \cos\Theta\mathbf{e}_x + \sin\Theta\cos\varepsilon\mathbf{e}_y + \sin\Theta\sin\varepsilon\mathbf{e}_z$.

The aerodynamic force $\mathbf{F}$ and torque $\mathbf{T}$ exerted on the sphere are found by integrating the stress vector $\mathbf{p}(\mathbf{n})$ and the torque surface density vector $R\mathbf{n}\times\mathbf{p}(\mathbf{n})$ over the sphere surface:

$$\mathbf{F} = R^2\int_0^{2\pi}\int_0^{\pi}\mathbf{p}(\mathbf{n})\sin\Theta\,d\Theta\,d\varepsilon, \qquad \mathbf{T} = R^3\int_0^{2\pi}\int_0^{\pi}\mathbf{n}\times\mathbf{p}(\mathbf{n})\sin\Theta\,d\Theta\,d\varepsilon, \tag{1.1}$$

where $\mathbf{a}\times\mathbf{b}$ is the vector product of the vectors $\mathbf{a}$ and $\mathbf{b}$.

Let $f(\mathbf{r},\ \mathbf{v})$ be the gas molecule velocity distribution function at an arbitrary point of the flow with the radius-vector $\mathbf{r}$ (here, $\mathbf{v}$ is the gas molecule velocity vector in the inertial reference frame considered) scaled to the gas molecule number concentration n ($n(\mathbf{r}) = \int f(\mathbf{r},\ \mathbf{v})\,d\mathbf{v}$). The stress vector $\mathbf{p}(\mathbf{n})$ can be expressed in terms of the values of $f(R\mathbf{n},\ \mathbf{v})$ at the point $\mathbf{r} = R\mathbf{n}$ on the sphere surface. For calculating $\mathbf{p}(\mathbf{n})$ it is convenient to use a local coordinate system which in the inertial reference frame has the velocity $\mathbf{V}_w(\mathbf{n}) = R\omega_s\times\mathbf{n}$. Then, the stress vector is determined as [22]

$$\mathbf{p}(\mathbf{n}) = -m\int\mathbf{n}\mathbf{v}^*\mathbf{v}^*f^*(R\mathbf{n},\ \mathbf{v}^*)\,d\mathbf{v}^*, \tag{1.2}$$

where, $\mathbf{v}^* = \mathbf{v} - \mathbf{V}_w(\mathbf{n})$, $f^*(R\mathbf{n},\ \mathbf{v}^*) = f(R\mathbf{n},\ \mathbf{v}^* + \mathbf{V}_w(\mathbf{n}))$, m is the gas molecule mass, and $\mathbf{ab}$ is the scalar product of the vectors $\mathbf{a}$ and $\mathbf{b}$.

The function $f(\mathbf{r},\ \mathbf{v})$ is a solution of the Boltzmann equation. The steady-state solution of this equation is found by the time relaxation method as the limit as $t\to\infty$ of the solution $f(\mathbf{r},\ \mathbf{v},\ t)$ of the nonstationary equation [22]

$$\frac{\partial f}{\partial t} + \mathbf{v}\frac{\partial f}{\partial\mathbf{r}} = I_B, \tag{1.3}$$

where I_b is the Boltzmann collision integral for rigid spheres with diameter d:

$$I_B = \frac{d^2}{2}\int\int_0^{2\pi}\int_0^{\pi}(f'f_1' - ff_1)|(\mathbf{v}_1 - \mathbf{v})\mathbf{d}|\sin\vartheta\,d\vartheta\,d\varphi\,d\mathbf{v}_1, \tag{1.4}$$

$$f = f(\mathbf{r},\ \mathbf{v},\ t), \quad f_1 = f(\mathbf{r},\ \mathbf{v}_1,\ t), \quad f' = f(\mathbf{r},\ \mathbf{v} + \mathbf{w},\ t), \quad f_1' = f(\mathbf{r},\ \mathbf{v}_1 - \mathbf{w},\ t),$$

$$\mathbf{w} = [(\mathbf{v}_1 - \mathbf{v})\mathbf{d}]\mathbf{d}, \qquad \mathbf{d} = \cos\vartheta\mathbf{e}_x + \sin\vartheta\cos\varphi\mathbf{e}_y + \sin\vartheta\sin\varphi\mathbf{e}_z.$$

The boundary conditions for (1.3) and (1.4) contain the condition on the sphere surface, where the distribution function of the molecules rebounding from the surface is found using the specular-diffusion reflection

model [22, 23]

$$\mathbf{v}\cdot\mathbf{n}\geq 0,\qquad f^*(R\mathbf{n},\,\mathbf{v}^*,\,t)=(1\,-\,\alpha_\tau)f^*(R\mathbf{n},\,\mathbf{v}^*\,-\,2(\mathbf{v}^*\mathbf{n})\mathbf{n},\,t)$$
$$+\,\alpha_\tau\frac{2}{\pi}\exp\left(-\frac{(\mathbf{v}^*)^2}{C_s^2}\right)\int\limits_{\mathbf{v}^{**}\atop\mathbf{n}<0}\frac{|\mathbf{v}^{**}\mathbf{n}|}{C_s^4}f^*(R\mathbf{n},\,\mathbf{v}^{**},\,t)\,d\mathbf{v}^{**}\quad(1.5)$$

(here, the relaxation temperature is taken equal to T_s) and the condition at points infinitely remote from the sphere, where the molecule distribution function is assumed to be equal to the Maxwellian equilibrium function:

$$|\mathbf{r}|\to\infty:\;\; f(\mathbf{r},\,\mathbf{v},\,t)\to f_\infty(\mathbf{v}),\qquad f_\infty(\mathbf{v})=\frac{n_\infty}{(\sqrt{\pi}C_\infty)^3}\exp\left(-\frac{(\mathbf{v}-\mathbf{U}_\infty)^2}{C_\infty^2}\right).\qquad(1.6)$$

In (2.5) and (1.6), $C_s=\sqrt{2k_BT_s/m}$, $C_\infty=\sqrt{2k_BT_\infty/m}$, k_B is the Boltzmann constant, and α_τ is the tangential-momentum accommodation coefficient ($0\leq\alpha_\tau\leq 1$), assumed to be constant. The value of α_tau depends on the gas species, the surface material, the roughness, the presence of impurities, and other factors. So, in practice, this coefficient is usually unknown. The typical value of α_τ is 0.9 [24]. Below, the coefficient α_τ is considered as a governing parameter of the problem, and a special investigation is performed to estimate the effect of its value on the calculation results.

For the limiting steady-state solution of problem (1.3)–(1.6), the initial condition at $t=0$ is arbitrary. In particular, as the initial condition we can use a uniform flow with the distribution function $f_\infty(\mathbf{v})$ over the entire flow region considered.

The solution of problem (1.3)–(1.6) in nondimensional form depends on six nondimensional similarity parameters. We can use, for instance, the following set of similarity parameters: the velocity ratio $S=U_\infty/C_\infty$ (U_∞ is the absolute value of the vector $\mathbf{U}_\infty$), the Knudsen number $\mathrm{Kn}=\lambda_\infty/R$ ($\lambda_\infty=1/(\sqrt{2}\pi d^2n_\infty)$) is the mean free path of the molecules-rigid spheres in the gas in the equilibrium state with the distribution function $f_\infty(\mathbf{v})$ [23], the temperature ratio T_s/T_∞, the angular velocity coefficient $W=R\omega_s/C_\infty$ (ω_s is the absolute value of the vector $\boldsymbol{\omega}_s$), the rotation angle Θ equal to angle between the vectors $\mathbf{U}_\infty$ and $\boldsymbol{\omega}_s$, and the accommodation coefficient α_τ.

As the similarity criterion, instead of S we can use the Mach number $\mathrm{M}=U_\infty/\sqrt{\gamma k_BT_\infty/m}=\sqrt{2/\gamma}S$ (γ is the gas specific heat ratio, $\gamma=5/3$ for a monatomic gas). In the continuum regime, the aerodynamic coefficients are usually considered as functions of the Reynolds number $\mathrm{Re}=2R\rho_\infty U_\infty/\mu_\infty$ ($\rho_\infty=mn_\infty$ and μ_∞ are the gas density and dynamic viscosity in the free stream) which can be used instead of the Knudsen number Kn. For a gas consisting of molecules-rigid spheres with the distribution function $f_\infty(\mathbf{v})$, the viscosity coefficient can be determined in the first approximation using the Chapman–Enskog method as $\mu_\infty=(5/16)\rho_\infty\lambda_\infty\sqrt{2\pi k_BT_\infty/m}$ [23]. There follows $\mathrm{Re}=(32/5)\sqrt{\gamma/2\pi}(\mathrm{M}/\mathrm{Kn})$. Instead of W, as the similarity parameter we can use the nondimensional angular velocity $\Omega=R\Omega_s/U_s=W/S$ [14] or the Reynolds number based on the angular velocity $\mathrm{Re}^2\rho_\infty\omega_s/\mu_\infty=\Omega\mathrm{Re}/2$ [18].

In the next two sections, we will consider the known data on the aerodynamics of a spinning sphere in the free-molecular ($\mathrm{Kn}\gg 1$) and continuum ($\mathrm{Kn}\ll 1$) flow regimes. These will be compared with the results of calculating the aerodynamic coefficients in the transitional ($\mathrm{Kn}=0.1$–10) and near-continuum ($\mathrm{Kn}=0.01$–0.1) flow regimes.

2. AERODYNAMIC COEFFICIENTS OF A SPINNING SPHERE IN THE FREE-MOLECULAR REGIME

In a free-molecular flow for $\lambda_\infty/R\gg 1$, the collision integral I_B in (1.3) can be set equal to zero. Then, in the steady-state free-molecular flow near a convex body the distribution function of the molecules colliding with the surface is equal to the free-stream function $f_\infty(\mathbf{v})$ [22] and the stress vector $\mathbf{p}(\mathbf{n})$ is obtained after

substituting (1.5) and (1.6) in (1.2):

$$\mathbf{p}(\mathbf{n}) = \mathbf{p}_n(\mathbf{n}) + \mathbf{p}_\tau(\mathbf{n}), \tag{2.1}$$

$$\mathbf{p}_n(\mathbf{n}) = p_\infty\left\{(\alpha_\tau - 2)\left[(1 + \operatorname{erf}(S_n))\left(S_n^2 + \frac{1}{2}\right) + \frac{S_n}{\sqrt{\pi}}\exp(-S_n^2)\right] - \frac{\alpha_\tau}{2}\chi(S_n)\frac{T_s}{T_\infty}\right\}\mathbf{n}, \tag{2.2}$$

$$\mathbf{p}_\tau(\mathbf{n}) = p_\infty\frac{\alpha_\tau\chi(S_n)}{\sqrt{\pi}}[S(\mathbf{e} - \mathbf{enn}) - W\mathbf{e}_\omega \times \mathbf{n}], \tag{2.3}$$

where $\mathbf{p}_n(\mathbf{n})$ and $\mathbf{p}_\tau(\mathbf{n})$ are the vectors of the normal and tangential stresses, $\mathbf{e}$ and $\mathbf{e}_\omega$ are the unit vectors directed along the vectors $\mathbf{U}_\infty$ and $\boldsymbol{\omega}_s$, $S_n = -S\mathbf{en}$, and $p_\infty = 1/2\rho_\infty C_\infty^2$, $\chi(x) = \exp(-x^2) + \sqrt{\pi}x[1 + \operatorname{erf}(x)]$, $\operatorname{erf}(x) = \frac{2}{\sqrt{\pi}}\int_0^x \exp(-y^2)\,dy$.

Using (2.1)–(2.3) for calculating $\mathbf{F}$ in (1.1), we obtain

$$\mathbf{F} = \mathbf{F}_D + \mathbf{F}_L, \tag{2.4}$$

$$\mathbf{F}_D = \frac{1}{2}\rho_\infty\pi R^2 C_D|\mathbf{V}_\infty - \mathbf{V}_s|(\mathbf{V}_\infty - \mathbf{V}_s), \quad \mathbf{F}_L = \frac{1}{2}\rho_\infty\pi R^3 C_L(\mathbf{V}_\infty - \mathbf{V}_s)\times\omega_s, \tag{2.5}$$

where $\mathbf{F}_D$ and $\mathbf{F}_L$ are the drag and Magnus forces and C_D and C_L are the drag and Magnus force coefficients given by the formulas

$$C_D = \frac{\exp(-S^2)}{\sqrt{\pi}S^3}(2S^2 + 1) + \frac{\operatorname{erf}(S)}{S^4}\left(2S^4 + 2S^2 - \frac{1}{2}\right) + \frac{2\alpha_\tau\sqrt{\pi}}{3S}\sqrt{\frac{T_s}{T_\infty}}, \tag{2.6}$$

$$C_L = -\frac{4}{3}\alpha_\tau. \tag{2.7}$$

The drag force coefficient in (2.6) is equal to the drag coefficient of a non-spinning sphere [25]. The coefficient C_L in form (2.7) was obtained in [10] for the case $\mathbf{U}_\infty\boldsymbol{\omega}_s = 0$ and in [11] for an arbitrary orientation of $\mathbf{U}_\infty$ and $\boldsymbol{\omega}_s$.

The aerodynamic torque T can be similarly obtained after substituting (2.1)–(2.3) in the definition of the torque (1.1):

$$\mathbf{T} = -\frac{1}{2}\rho_\infty\pi R^5\omega_s^2(C_T\boldsymbol{e}_\omega + C_{T\perp}\mathbf{e}_{\omega\perp}), \qquad \mathbf{e}_{\omega\perp} = \frac{\mathbf{e} - (\mathbf{ee}_\omega)\mathbf{e}_\omega}{|\mathbf{e} - (\mathbf{ee}_\omega)\mathbf{e}_\omega|}, \tag{2.8}$$

where C_T and $C_{T\perp}$ are the coefficients of the aerodynamic-torque components directed parallel and normal to the vector $\boldsymbol{\omega}_S$

$$C_T = -\frac{\alpha_\tau}{\sqrt{\pi}W}[I_1 + I_2 + (I_2 - 3I_1)(\mathbf{ee}_\omega)^2], \tag{2.9}$$

$$C_{T\perp} = -\frac{\alpha_\tau}{\sqrt{\pi}W}(I_2 - 3I_1)(\mathbf{ee}_\omega)|\mathbf{e} - (\mathbf{ee}_\omega)\mathbf{e}_\omega|, \tag{2.10}$$

$$I_1 = \frac{\sqrt{\pi}}{2}\frac{\operatorname{erf}(S)}{S^3}\left(S^4 + \frac{1}{4}\right) + \frac{\exp(-S^2)}{2S^2}\left(S^2 - \frac{1}{2}\right),$$

$$I_2 = \sqrt{\pi}\frac{\operatorname{erf}(S)}{S}\left(S^2 + \frac{1}{2}\right) + \exp(-S^2).$$

In accordance with (2.8)–(2.10), the vector $\mathbf{T}$ lies in the plane of the vectors $\mathbf{U}_\infty$ and $\boldsymbol{\omega}_s$; however, it is parallel to the vector $\boldsymbol{\omega}$ only when the vectors $\mathbf{U}_\infty$ and $\boldsymbol{\omega}_s$ are either parallel or perpendicular to each other. Relations (2.8)–(2.10) were first obtained in [11] in another mathematical form.

3. AERODYNAMIC COEFFICIENTS OF A ROTATING SPHERE IN THE CONTINUUM FLOW REGIME

The known data on the aerodynamic coefficients of a spinning sphere in the continuum flow regime relate mainly to two particular cases, when either the vectors $\mathbf{U}_\infty$ and $\boldsymbol{\omega}_s$ are perpendicular to each other ($\Theta = 90\%$) or the sphere rotates in a quiescent gas ($\mathbf{U}_\infty = 0$). Under these conditions, the aerodynamic force can be represented in the form $\mathbf{T} = -(1/2)\rho_\infty \pi R^5 C_T \omega_s \boldsymbol{\omega}_s$.

In a uniform incompressible flow past a non-spinning sphere, the drag force coefficient depends only on the Reynolds number. Different approximations of the dependence $C_D(\mathrm{Re})$ were analyzed in [9]. A fairly simple approximation ensuring sufficient accuracy for many applications was proposed in [2]. The effects of compressibility and rarefaction on the drag coefficient were studied experimentally in [3–6]. In [7] a system of relations for calculating C_d in the free-molecular, transitional, and continuum flow regimes for $\mathrm{M} < 6$ and $\mathrm{Re} < 10^5$ was proposed. This system is accepted as one of the best, although, for the transonic regime it gives a calculation error for C_d of about 16% [8].

In [1] it was shown that in the continuum flow regime at small Reynolds numbers the rotation does not affect the drag force coefficient. The effect of sphere rotation on the drag force coefficient in an incompressible flow for $100 \le \mathrm{Re} \le 300$ was studied numerically in [12]. It was shown that C_d increases slowly with increase in $\boldsymbol{\Omega}$ in accordance with the approximate formula

$$C_D = C_{D0}(1 + \Omega)^{\mathrm{Re}/1000}. \tag{3.1}$$

where C_{D0} is the drag force coefficient of a non-spinning sphere.

The Magnus force acting on a non-spinning sphere in the continuum regime has been studied only for incompressible flows. For flows at small Reynolds numbers ($Re \ll 1$ and $Re_\omega \ll 1$) it was found theoretically in [1] that $C_L = 2$. From the comparison of this value with (2.7) it is clear that in a continuum flow at small Reynolds numbers and in a free-molecular flow the Magnus force acts in opposite directions. The Magnus force coefficient at finite Reynolds numbers was studied in [12–17]. It was found that C_L decreases with increase in Re and that, for large Reynolds numbers, the value of this coefficient depends mainly on Ω. Thus, in [14] the following approximation was proposed:

$$C_L = \frac{1}{\Omega}[0.45 + (2\Omega - 0.45)\exp(-0.075\Omega^{0.4}\mathrm{Re}^{0.7})]. \tag{3.2}$$

This approximation is valid for $2\Omega \ge 0.45$ and $10 \le \mathrm{Re} \le 140$. From (3.2) it follows that $C_L \to 0.45/\Omega$ as $\mathrm{Re} \to \infty$. This agrees with the experimental data for large Reynolds numbers [15]. However, in [12] on the basis of calculations it was found that C_L is almost independent of Re for $0.16 \le \Omega \le 0.5$ and $100 \le \mathrm{Re} \le 300$, and the dependence on Ω can be approximated by the formula

$$C_L = \frac{0.11}{\Omega}(1 + \Omega)^{3.6}. \tag{3.3}$$

According to the results obtained by the authors, the error of this formula amounts to 20%. Formulas (3.2) and (3.3) predict different dependences of C_L on Ω. However, the experimental values of C_L obtained by different authors also differ substantially from each other [16]. Apparently, the dependence of C_L on the similarity criteria is fairly complex, and so far no semi-empirical formulas valid for calculating C_L over a wide range of the governing parameters [16] have been proposed.

The torque coefficient of a spinning sphere in Stokes flow ($\mathrm{Re}_\omega \ll 1$) was found in [26] in the form $C_T = 16\pi/\mathrm{Re}_\omega$. In [1], it was shown that this result is also valid in the Oseen approximation for the translational motion of a sphere relative to the fluid. At finite Reynolds numbers Re_ω, the torque coefficient appears to have been studied only for a sphere spinning in a quiescent incompressible fluid. In [18], on the basis of an analysis of the data of different authors, several approximations for C_T were proposed; these can

be combined in the single relation:

$$C_T = \frac{1}{\mathrm{Re}_\omega} \times \begin{cases} 16\pi, & \mathrm{Re}_\omega < 6.03; \\ 37.2 + 5.32\sqrt{\mathrm{Re}_\omega}, & 6.03 \le \mathrm{Re}_\omega \le 20.37; \\ 32.1 + 6.45\sqrt{\mathrm{Re}_\omega}, & 20.37 \le \mathrm{Re}_\omega < 40000. \end{cases} \tag{3.4}$$

4. NUMERICAL METHOD AND GOVERNING PARAMETERS

The flow and the aerodynamic coefficients were calculated by the method of direct statistical simulation based on the Bird NTC scheme [23]. As is well known [27, 28], this method can be regarded as a numerical procedure for estimating the functionals of the solutions of the Boltzmann kinetic equation (1.3), (1.4). In the calculations, we used a rectangular calculation domain with a spinning sphere located at the center. In calculating the subsonic flows, the boundaries of the calculation domain were located at a distance of (20–40)R from the sphere surface.

For verifying the algorithm, we performed test calculations in which we varied all the numerical parameters (time step, grid cell size, etc.) These calculations, some of whose results were presented in [29], made it possible to justify the choice of the parameters of the numerical algorithm, which is particularly important for modeling subsonic flows. For the parameters chosen, in the framework of the model used the maximum calculation error for the aerodynamic coefficients did not exceed 10% for $\mathrm{Kn} < 0.4$, $\mathrm{M} < 0.6$ and 7% for $\mathrm{Kn} < 0.1$ and $\mathrm{M} \ge 1$. In other cases, the error typically did not exceed 3–5%.

We performed a series of preliminary calculations in which we varied the temperature ratio T_s/T_∞. The calculations demonstrated that the variation of T_s/T_∞ over a relatively narrow range (for instance, $0.8 < T_s/T_\infty < 1.2$ for $\mathrm{M} = 0.2$) has only a weak impact on the aerodynamics of the sphere. At the same time, when T_s/T_∞ is varied over a broader range the velocity and temperature fields may be fairly different and their interrelation requires detailed analysis. The calculation of these flows may require the use of other models which more adequately describe the physics of intermolecular collisions and the interactions of the molecules with the body surface over a wide range of variation of the temperature, as compared with the models used in this paper. These questions could constitute the subject of a special investigation.

For these reasons, in the calculations described below we assume that $T_s/T_\infty = 1$, the other similarity parameters M, Kn, W, Θ, and α being varied. We investigated flows with the Mach numbers 0.1, 0.2, 0.6, 1, 1.5, and 2. The Knudsen number was varied from 0.05 to 20 for $\mathrm{M} < 1$ and from 0.025 to 20 for $\mathrm{M} \ge 1$. The angular velocity coefficient W was varied from 0.03 to 6 for $\mathrm{M} < 1$ and to 8 for $\mathrm{M} \ge 1$, the angle Θ was varied from 0 to 180°, and the accommodation coefficient α_τ from 0 to 1. Most of the calculations in which the dependence of the aerodynamic coefficients on the Knudsen number was studied were performed for $\Theta = 90\%$and $\alpha_\tau = 1$. Most of the results were obtained for W varying from 0.1 to 1. This range is of interest, for instance, for calculating the aerodynamic coefficients of dispersed particles in supersonic gas-particle flows.

In the calculations, we found all six of the aerodynamic coefficients of the sphere corresponding to the projections of the aerodynamic drag force **F** and the torque **T** on the axes of the Cartesian coordinate system in Fig. 1.

5. DRAG FORCE COEFFICIENT OF A SPHERE

The results of the calculations of C_D are shown in Fig. 2 together with the experimental data [5] and also the values of C_D obtained using the formulas in [7] (denoted below by C_D^H) and [2]. Curves *1* and *2* correspond to the case of a spinning sphere. However, on curve *1* the values differ from C_D for $W = 0$ by not more than 4%.

As $\mathrm{Kn} \to \infty$, the values of C_D tend to the values of the drag coefficient obtained using (2.6) (straight lines *7*). For $T_s/T_\infty = 1$ and $\mathrm{M} = \mathrm{const} \le 1$, we have: $C_d^H \to C_{D(0)}^H \approx 4.07/S + 0.6S$ as $\mathrm{Re} \to 0$. The limiting values $C_{D(0)}^H$ are fairly close to the drag coefficient obtained using (2.6) for $\alpha_\tau = 0.9$ and $T_s/T_\infty = 1$. For

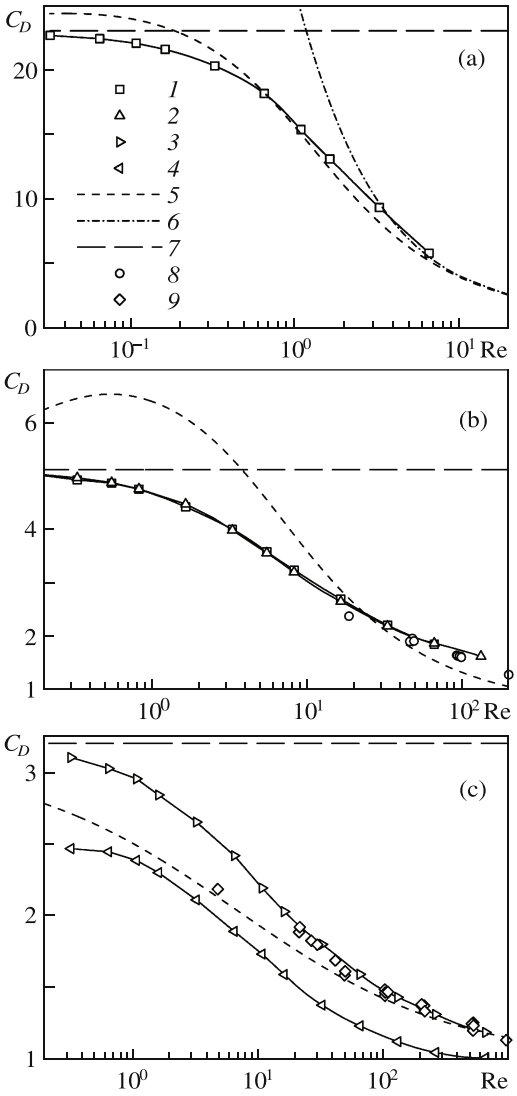

Fig. 2. Sphere drag force coefficient C_D as a function of Re for M = 0.2 (a), 1 (b), and 2 (c). Curves (*1–4*) correspond to the numerical results, (*5*) to formulas [7], (*6*) to [2], (*7*) to (2.6), (*8*, *9*) to the experimental data [5]: (*1*), (*2*), (*3*), (*7*) $\alpha_\tau = 1$; (*4*) $\alpha_\tau = 0$; (*1*) W = 0.1, $\Theta = 90^\circ$; (*2*) W = 1, $\Theta = 90^\circ$; (*3*) W = 0; (*8*) $1.003 \le M \le 1.19$; (*9*) $1.9 \le M \le 2.2$.

example, $C_D \approx 22.35$, $C^H_{D(0)} \approx 22.4$ for M = 0.2. However, over the range of small Reynolds numbers the dependence of C^H_D on Re is nonmonotonic (Fig. 2b) and C^H_D tends to $C^H_{D(0)}$ comparatively slowly. Due to this, the maximum difference between the calculated values of the drag force coefficient C^H_D is observed on the boundary between the free-molecular and transitional flow regimes for Kn ~ 10. We can assume that the nonmonotonicity of the function $C^H_D(\mathrm{Re})$ is a defect of the approximations [7]. Unfortunately, we did not find any experimental data on the drag force coefficient of a sphere for $0.1 \le M \le 0.6$ and Kn > 0.1.

In a subsonic flow (M = 0.2, Fig. 2a) the values of C_D and C^H_D agree well for Kn ≤ 2. In the transitional and near-continuum flow regimes C_D and C^H_D differ most strongly for transonic flow past the sphere (Fig. 2b). For M ≥ 1 about half the points from [5] lie nearer to the calculated curves C_D than to C^H_D. For Kn ≤ 0.6, the value of C_D differs from C^H_D by not more than 10%, and the difference between C_D and the points from [5] (if one point, which "drops out" in Fig. 2c, is excluded from consideration) does not exceed 7%. The difference between the values of C^H_D and the experimental data [5] lies within the range from 4% to 16% [8]. Hence, the difference between C_D and C^H_D lies within the limits of error of the formulas [7]. We also calculated the drag coefficients of a non-spinning sphere for M = 2, $2 \times 10^{-2} \le \mathrm{Kn} \le 5 \times 10^{-4}$ and $\alpha_\tau = 1$. On this range of Kn, the values of C_D differ from C^H_D by not more than 10%.

Thus, the drag coefficients calculated agree satisfactorily both with the data of physical experiments and the known semi-empirical formulas.

6. EFFECT OF THE ACCOMMODATION COEFFICIENT ON THE AERODYNAMIC COEFFICIENTS

A comparison of *3* and *4* in Fig. 2c shows that a decrease in the accommodation coefficient α_τ results in a decrease in C_D. In the transitional regime, the values of C_D for $\alpha_\tau = 1$ also turned out to be slightly greater than C_D^H and some of the points from [5]. It turned out that to achieve agreement between C_D and C_D^H in the transitional flow regime, it is necessary to take the value of α_τ on the range 0.7–0.9. It is difficult, by comparing C_D and C_D^H, to estimate exactly a value of the accommodation coefficient which can be recommended for subsequent calculations, because when α_τ is varied from 0.8 to 1 the variation of C_D is of the same order as the difference between C_D^H and the experimental values from [5].

In accordance with the formulas (2.6), (2.7), (2.9), and (2.10), in a free-molecular flow all the aerodynamic coefficients of a spinning sphere are linear functions of the accommodation coefficient. To clarify the form of this dependence in the transitional flow regime, we performed calculations in which the value of α_τ was varied from 0 to 1 and the other parameters corresponded to all possible combinations of the following values: M = 0.1, 0.2, 0.6, 1, 1.5 and 2; Kn = 10, 1, and 0.2–0.1; W = 0.1 and 1; and $\Theta = 90^\circ$. An analysis of the results demonstrated that in the first approximation all the aerodynamic coefficients also depend linearly on α_τ (an example of these dependences obtained for M = 1 is given in [29]), i.e.

$$C_D \approx C_{D(0)} + \alpha_\tau(C_{D(1)} - C_{D(0)}), \quad C_L \approx \alpha_\tau C_{L(1)}, \quad C_T \approx \alpha_\tau C_{T(1)}, \tag{6.1}$$

where $C_{D(a)}$, $C_{L(a)}$, and $C_{T(a)}$ are the values of the corresponding aerodynamic coefficients for $\alpha_\tau = a$. Thus, the effect of the accommodation coefficient on all the aerodynamic coefficients of the spinning sphere in the transitional flow regime is almost the same as in the free-molecular regime. It is sufficient to study the coefficients of the Magnus force and the aerodynamic torque for $\alpha_\tau = 1$ only, while their values for other values of α_τ can be estimated using (6.1).

In the transitional flow regime, the value of α_τ not only affects the flow near the sphere surface but also determines the global flow pattern. In particular, for M = 2, Kn = 0.01, and W = 0 in the case of the specular-reflection model ($\alpha_\tau = 0$) the length of the ring vortex region attached to the trailing surface of the sphere in the direction of the undisturbed flow is almost half the length of this region for the diffusion reflection model ($\alpha_\tau = 1$) [29].

7. DEPENDENCE OF THE AERODYNAMIC COEFFICIENTS OF THE SPHERE ON THE ROTATION ANGLE

For an arbitrary value of the angle Θ the aerodynamic force and torque can be represented in the form:

$$\mathbf{F} = \frac{1}{2}\rho_\infty \pi R^2 U_\infty [U_\infty C_D \mathbf{e}_x + R\omega_s(C_y \mathbf{e}_y + C_z \mathbf{e}_z)],$$

$$\mathbf{T} = -\frac{1}{2}\rho_\infty \pi R^5 \omega_s^2 (C_{Tx}\mathbf{e}_x + C_{Ty}\mathbf{e}_y + C_{Tz}\mathbf{e}_z),$$

where C_y and C_z are the coefficients of the lift force and the Magnus force, C_{Tx}, C_{Ty}, and C_{Tz} are the corresponding coefficients of the aerodynamic torque.

From (2.5), (2.6), (2.9), and (2.10), it follows that in a free-molecular flow the following formulas hold [11]: $C_y = 0$, $C_z = C_L \sin\Theta$, $C_{Tx} = 2\alpha_\tau/(\sqrt{\pi}W)(I_2 - I_1)\cos\Theta$, $C_{Ty} = \alpha_\tau/(\sqrt{\pi}W)(I_2 - I_1)\sin\theta$, $C_{Tz} = 0$. To clarify the dependence of the aerodynamic coefficients on Θ, we performed calculations in which the angle Θ was varied from 0 to 180°, while the other parameters corresponded to all possible combinations of the values: M = 0.1, 0.2, 0.6, 1, 1.5, and 2; Kn = 10, 1, and 0.1–0.2; W = 0.1 and 1; and $\alpha_\tau = 1$. Typical

calculations of the coefficients C_D, C_y, C_z, C_{Tx}, and C_{Ty} as functions of the angle Θ in the transitional flow regime are presented in Fig. 3. The data for the coefficient C_{Tz} are not plotted in Fig. 3 because in all the calculations the value of C_{Tz} turned out to be less than 0.2% of C_T, i.e. less then the calculation error. In Fig. 3a, the values of C_y are not shown because the values of C_y calculated for subsonic flows also turned out to be less than the calculation accuracy. The curves in Fig. 3 were plotted using the formulas:

$$C_D(\Theta) = C'_D + (C''_D - C'_D)\frac{1+\cos(2\Theta)}{2}, \quad C_y(\Theta) = C'''_y \sin(2\Theta), \tag{7.1}$$

$$C_z(\theta) = C'_L \sin\Theta, \quad C_{Tx}(\Theta) = C''_T \cos\Theta, \quad C_{Ty} = C'_T \sin(\Theta), \tag{7.2}$$

where C'_D, C'_L, and C'_T are the calculated values of the aerodynamic coefficients for $\Theta = 90^\circ$, C''_D and C''_T those for $\theta = 0$, and C'''_y that for $\Theta = 45^\circ$. As is clear from Fig. 3, the calculation results agree very well with simple approximations (7.1) and (7.2). Accordingly, it is sufficient to study numerically only the aerodynamic coefficients C'_D, C'_L, C'_T, C''_D, C''_T, and C'''_y for the corresponding values of the angle Θ.

Thus, the functional dependence of the coefficients C_z, C_{Tx}, and C_{Ty} on Θ in the transitional regime takes practically the same form as in the free-molecular regime. In all our calculations, the drag force coefficient varied fairly weakly with Θ ($C''_D \approx C'_D$) and the maximum value of the lifting force coefficient C'''_L amounted to about 10% of $|C_L|$. Because of this, in varying the other governing parameters attention was focused on the calculation of the aerodynamic coefficients C'_D, C'_L, and C'_T for $\Theta = 90^\circ$.

For small values of the Mach number (Fig. 3a), we have $C''_T \approx C'_T$ and, moreover, $C_{Tx}(\Theta) \approx C_{Ty}(90^\circ - \Theta)$ for $\Theta \le 90^\circ$. Hence, in subsonic flow past the sphere the value of $C_{T\perp}$ is fairly small. In supersonic flow (Fig. 3b), the value of C_d decreases slightly with increase in Θ from 0 to 90°, and $C''_T < C'_T$, so that in this case there may be a certain difference in the directions of the vectors $\boldsymbol{\omega}_s$ and $\mathbf{T}$.

8. MAGNUS FORCE COEFFICIENT

The calculated values of the Magnus force coefficient C_L are presented in Fig. 4 as functions of Kn and Re for several constant values of M and W and hence a constant nondimensional angular velocity $\Omega = \sqrt{2/\gamma}\mathrm{W}/\mathrm{M}$. For comparison, in Fig. 4b we have also plotted the dependences $C_L(\mathrm{Re})$ obtained using formula (3.2) for the continuum flow regime. With decrease in Kn, in subsonic flow the coefficient C_L varies from the value $-4/3$ in the free-molecular flow to positive values in the transitional and near-continuum flow regimes. The critical values Re_* and Kn_* at which C_L vanishes (i.e. $C_L(\mathrm{Re}_*, \mathrm{M}, \mathrm{W}) = 0$) are presented in Fig. 5 for $\mathrm{W} = 0.1$. The calculation results show that Re_* and Kn_* depend only slightly on W for $0.1 \le \mathrm{W} \le 0.5$. The critical Knudsen number decreases almost linearly with increase in M. For $\mathrm{M} \ge 1.5$, in all our calculations the Magnus force coefficient remained negative. This fact agrees with the results of calculating the lift force on a rotating circular cylinder immersed in a cross-flow of rarefied gas [30]. The form of the curves *6* and *7* in Fig. 4 makes it possible to assume that in supersonic flows for $\mathrm{M} \ge 1.5$ and $\mathrm{W} \le 1$ the value of C_L also remains negative for Knudsen numbers corresponding to continuum flow.

Curves *8–10* in Fig. 4b correspond to the values of C_L for vanishingly small values of M and Kn. However, for any small but finite Mach number the values of C_L should tend to $-4/3$ as $\mathrm{Kn} \to \infty$. This means that for $\mathrm{M} = \mathrm{const} \ll 1$ the functions $C_L(\mathrm{Kn})$ and $C_L(\mathrm{Re})$ are nonmonotonic. With decrease in Kn, the value of C_L should first increase from $-4/3$ to the maximum value of 2 corresponding to the continuum flow regime at small Reynolds numbers and then decrease to the limiting value corresponding to large Reynolds numbers. It is natural to assume that the nonmonotonic dependence of C_L on Kn is also preserved for those Mach numbers at which the compressibility is significant; however, the maximum value of C_L turns out to be less than 2. The calculation results agree with the hypothesis of nonmonotonicity of the dependence $C_L(\mathrm{Kn})$. Over the range of Mach numbers considered, the Knudsen number $\mathrm{Kn}_{\max}$, at which C_L is maximum, is less than 0.05. The calculated values of C_L can be approximated by the formula

$$C_L(\mathrm{M}, W, \mathrm{Kn}) = C_{Lt}(\mathrm{M}, W)\frac{1-F(\mathrm{Kn})}{1-F_t} + C_{L\infty}\frac{F(\mathrm{Kn})-F_t}{1-F_t}. \tag{8.1}$$

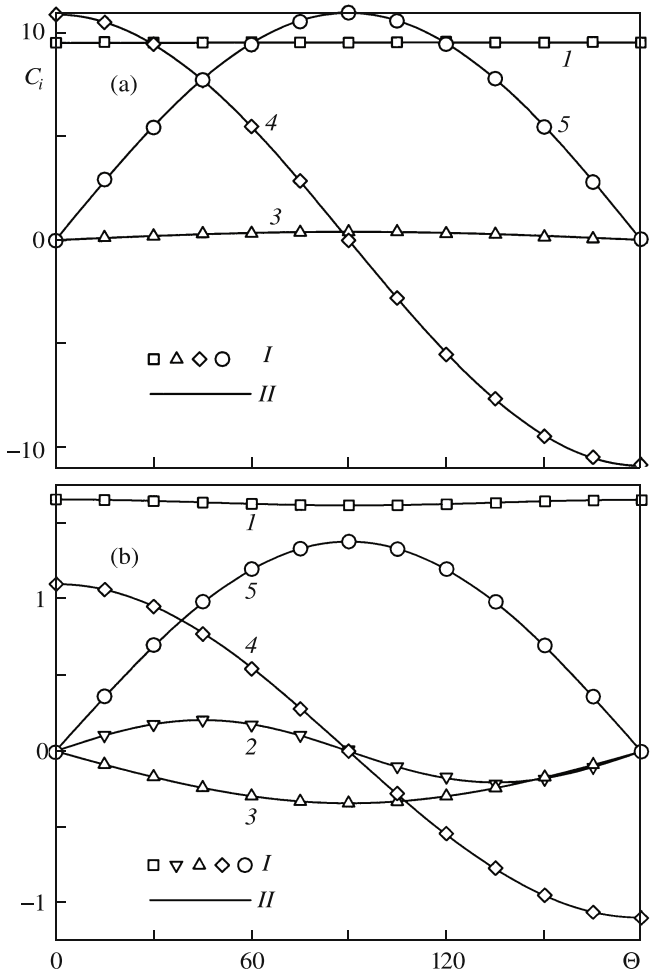

Fig. 3. Aerodynamic coefficients of a sphere obtained from numerical calculations (*I*) and the formulas (7.1), (7.2) (*II*) as functions of the rotation angle Θ for M = 0.2, Kn = 0.2, W = 0.1 (a) and M = 2, Kn = 0.1, W = 1 (b): (*1*) C_D; (*2*) $C_y \times 10$; (*3*) C_z; (*4*) C_{Tx}; (*5*) C_{Ty}, $\alpha_\tau = 1$.

where $F(\mathrm{Kn})$ is a certain function of Kn, such that $F \to 1$ as $\mathrm{Kn} \to \infty$ and $F \to -1$ as $\mathrm{Kn} \to 0$, $C_{Lt}(\mathrm{M}, W)$ is the dependence of C_L on M and W for Kn_t ($\mathrm{Kn}_t > \mathrm{Kn}_{\max}$), $C_{L\infty} = -4/3$, and $F_t = F(\mathrm{Kn}_t)$. Satisfactory results can be obtained for $\mathrm{Kn}_t = 0.1$, $F(\mathrm{Kn}) = \mathrm{erf}[\log(\mathrm{Kn}/0.37)]$ (then $F_t \approx -0.578$) using as $C_{Lt}(\mathrm{M}, W)$ the function

$$C_{Lt}(\mathrm{M}, \mathrm{W}) = -(0.06 + 0.14 \times \mathrm{M}) \times [1 - s(\mathrm{M})] + [(1.1 - 1.16 \times \mathrm{M}) \times (1 - W)] + (0.78 - 0.87 \times \mathrm{M}) \times (\mathrm{W} - 0.1) - 0.03 \sin(2\pi \mathrm{M}) \times s(\mathrm{M}), \quad (8.2)$$

$$s(\mathrm{M}) = s_*(10 \times \mathrm{M} - 10.5), \quad (8.3)$$

$$s_*(\zeta) = \eta(\zeta)\eta(1 - \zeta)[1 - \zeta^2(3 - 2\zeta)], \qquad \eta(\zeta) = \begin{cases} 1, & \zeta \geq 0; \\ 0, & \zeta < 0. \end{cases} \quad (8.4)$$

Relations (8.1)-(8.4) approximate the data of the numerical calculations of the Magnus force coefficient for $\mathrm{Kn} > 0.05$, $0.1 \leq \mathrm{M} \leq 2$, $0.1 \leq W \leq 1$, $T_s/T_\infty = 1$, $\Theta = 90^\circ$, and $\alpha_\tau = 1$. From (7.2) it follows that C_L is almost independent of Θ. The value of C_L for other α_τ can be estimated using (6.1). The values calculated using formulas (8.1)-(8.4) are represented for comparison by curves *III* in Fig. 4,a. Their mean-square deviation from the numerical calculations amounted to 3% of $|C_{L\infty}|$, with the maximum deviation being equal to 7%.

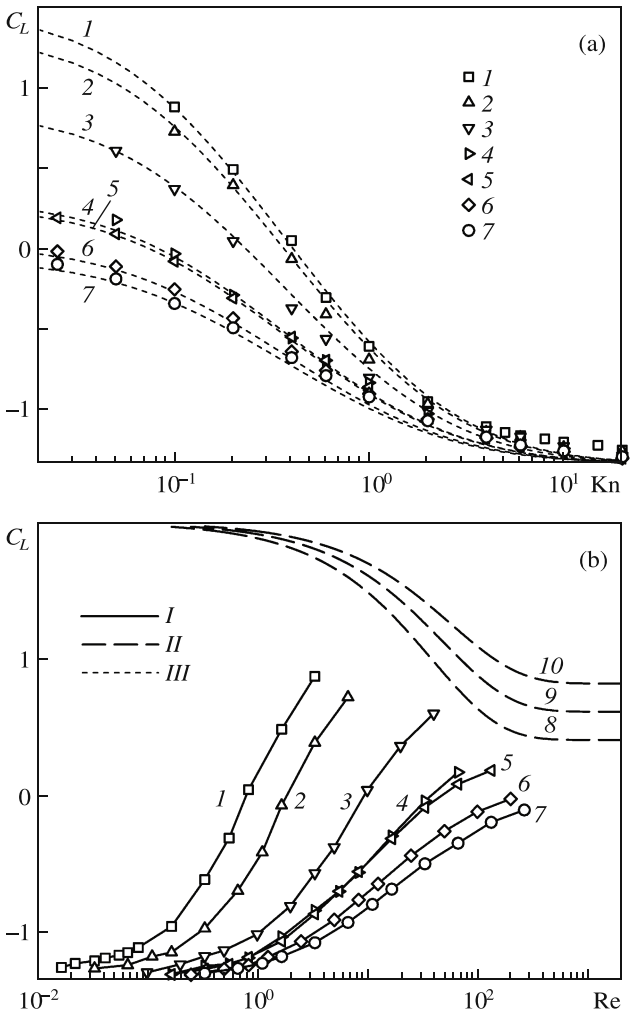

Fig. 4. Magnus force coefficient C_L as a function of Kn (a) and Re (b) found from numerical calculations (*I*); using formula (3.2) (*II*); and formulas (3.4) (*III*): *1–4* subsonic flow, W = 1; *5–7* supersonic flow, W = 1; *8–10* incompressible continuum flow; (*1*) M = 0.1, (*2*) 0.2, (*3*) 0.6, (*4*), (*5*) 1; (*6*) 1.5, (*7*) 2, (*8*) $\Omega \approx 1.1$, (*9*) 0.73, (*10*) 0.55, $\Theta = 90^\circ$, $\alpha_\tau = 1$.

Due to the above-mentioned nonmonotonicity of the dependence $C_L(\mathrm{Kn})$, for constructing universal dependences for the Magnus force coefficient valid for the free-molecular, transitional, and continuum flow regimes, it is not sufficient to use relations (8.1)-(8.4) together with the formulas for the continuum flow regime, for example (3.2) or (3.3). To obtain universal dependences it is necessary to have the data for the Magnus force in compressible-gas flows at Knudsen numbers of the order of 0.01.

The change in the sign of C_L and hence the direction of the Magnus force reflects the law of transformation of the stress distribution with variation of the Knudsen number. The Magnus force coefficient can be represented in the form $C_L = C_{L(n)} + C_{L(\tau)}$, where $C_{L(n)}$ and $C_{L(\tau)}$ are the fractions of C_L created by the distributions of the normal $\mathbf{p}_n$ and tangential $\mathbf{p}_\tau$ stresses. For $\Theta = 90^\circ$ they can be determined as

$$C_{L(\xi)} = \frac{F_{L(\xi)}}{F_L^*}, \qquad F_{L(\xi)} = R^2 \int_0^{2\pi} \int_0^{\pi} \mathbf{e}_z \mathbf{p}_\xi(\mathbf{n}) \sin\theta \, d\theta \, d\varepsilon,$$

where $F_L^* = p_\infty \pi R^2 \mathrm{SW}$, $\xi = n, \tau$. The stress fields $p_{nz} = \mathbf{e}_z \mathbf{p}_n$ and $p_{\tau z} = \mathbf{e}_z \mathbf{p}_\tau$ on the surface of a spinning sphere were analyzed in [21, 29]. In free-molecular flow, in accordance with (2.2) the quantity p_{nz} is odd with respect to the angle ε $(p_{nz}(\theta, -\varepsilon)) = -p_{nz}(\theta, \varepsilon)$, and hence $C_{L(n)} = 0$, $C_L = C_{L(\tau)} < 0$. In the transitional flow regime, the p_{nz} field ceases to be odd with respect to ε. In the neighborhood of the point

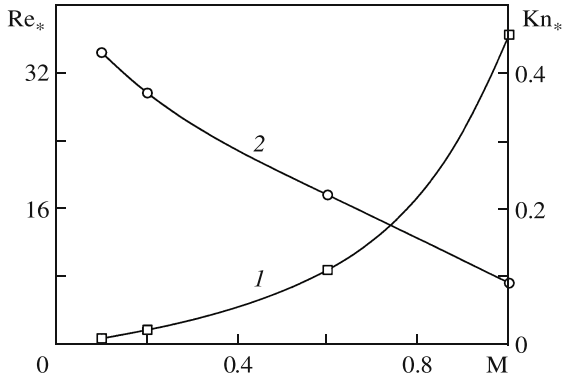

Fig. 5. Critical numbers Re_* (*1*) and Kn_* (*2*) as functions of M for W = 0.1.

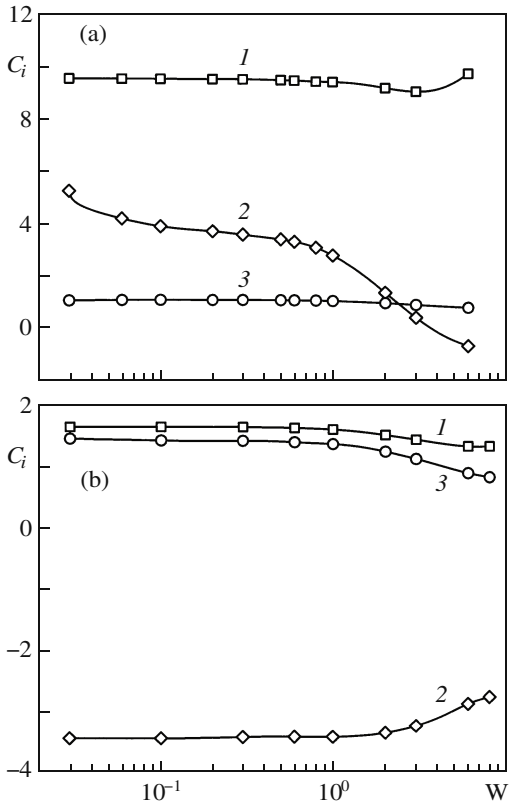

Fig. 6. Aerodynamic coefficients of a sphere as functions of the angular velocity coefficient W for M = 0.2, Kn = 0.2 (*1*) and M = 2, Kn = 0.1 (*b*): (*1*) C_D; (*2*) $C_L \times 10$; (*3*) $C_T \times \mathrm{W}$, $\Theta = 90^\circ$, $\alpha_\tau = 1$.

$\theta = 90^\circ$, $\varepsilon = 90^\circ$ the absolute value $|p_{nz}|$ (Fig. 1) turns out to be always smaller than the value of $|p_{nz}|$ at the symmetric point $\theta = 90^\circ$, $\varepsilon = 270^\circ$. As a result, in the transitional regime the contribution of the normal stresses is always positive: $C_{L(n)} > 0$. The variation of the tangential-stress field $p_{\tau z}$ in the transitional regime is much more complex than in the free-molecular regime. With decrease in Kn, the absolute value of $p_{\tau z}/p_\infty$ generally decreases, hence the contribution of the tangential stresses $C_{L(\tau)}$ also decreases in absolute value. As a result, the sum $C_{L(n)} + C_{L(\tau)}$ changes sign at a certain Knudsen number. Some calculated values of $C_{L(n)}$ and $C_{L(\tau)}$ and also the fractions of the drag force coefficient $C_{D(n)}$ and $C_{D(\tau)}$ are given in the Table for $\Theta = 90^\circ$ and $\alpha_\tau = 1$.

Thus, the change in the sign of C_L and in the Magnus force direction in the transitional flow regime is attributable to the increase in the contribution of the normal stresses to the Magnus force with decrease in Kn.

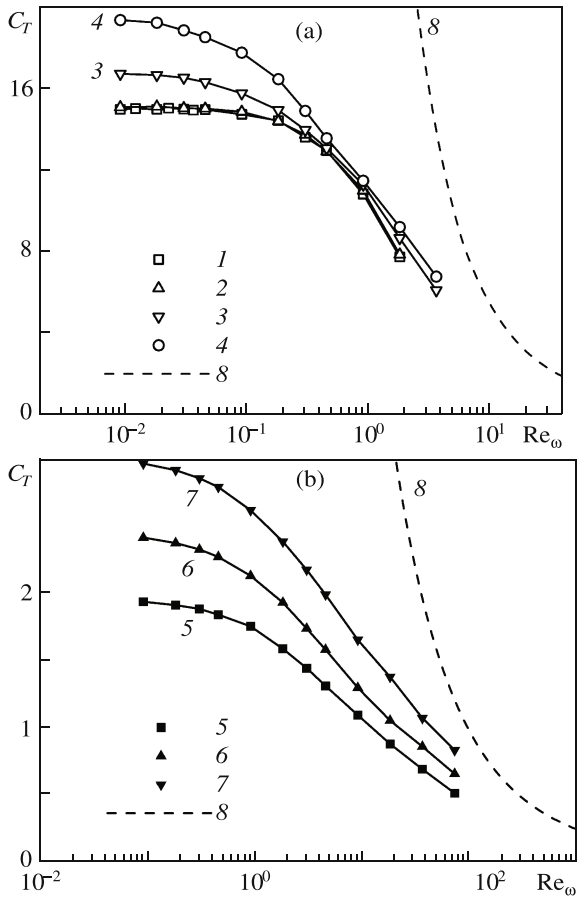

Fig. 7. Aerodynamic-torque coefficient of a sphere C_T as a function of Re_ω obtained from numerical calculations in the transitional regime (*1–7*) and using formula (3.4) in the continuum flow regime (*8*) for subsonic (a) and supersonic (b) flows: (*1–4*) W = 0.1; (*5–7*) W = 1; (*1*) M = 0.1; (*2*) 0.2, (*3*) 0.6, (*4*), (*5*) 1, (*6*) 1.5, (*7*) 2, $\Theta = 90^\circ$, $\alpha_\tau = 1$.

Table

No.	W	C_D	$C_{D(n)}$	$C_{D(\tau)}$	C_L	$C_{L(n)}$	$C_{L(\tau)}$	Ω	Re	Re_ω
M = 0.2, Kn = 0.2,	0.1	9.52	5.09	4.43	0.39	0.45	−0.06	0.55	3.23	0.89
	3	9.02	3.25	5.77	0.04	0.15	−0.11	16.4	3.23	26.5
M = 2, Kn = 0.1	0.1	1.66	1.18	0.48	−0.34	0.12	−0.46	0.055	64.7	1.78
	6	1.34	0.72	0.62	−0.29	0.04	−0.33	3.28	64.7	106

9. EFFECT OF THE ANGULAR VELOCITY COEFFICIENT ON THE AERODYNAMIC COEFFICIENTS OF THE SPHERE

To clarify the dependence of the aerodynamic coefficients on W, we performed calculations in which the value of W was varied from 0.03 to 6–8, with the other governing parameters being obtained as combinations of the following values: M = 0.1, 0.2, 0.6, 1, 1.5, and 2; Kn = 10, 1 and 0.1–0.2; $\Theta = 90^\circ$; $\alpha_\tau = 1$. Typical dependences of the aerodynamic coefficients on W in the transitional flow regime are presented in Fig. 6a and 6b for sub- (M = 0.2) and supersonic (M = 2) flow past the sphere, respectively. Figure 6 shows that the values of C_D, C_L, and $C_T \times \mathrm{W}$ depend comparatively weakly on W on the range $0.1 \le \mathrm{W} \le 1$. To understand more clearly the trend in the variation of these parameters with increase in W, we performed methodical calculations for large values of W.

With increase in W, for sub- and supersonic flow velocities the coefficients C_D and C_T vary in a qualitatively similar manner. The torque coefficient is approximately inversely proportional to W, which is similar

both to its behavior in the free-molecular flow (in accordance with (2.9)) and to its dependence on Re_ω in the continuum regime (in accordance with (3.4)).

In contrast to (3.1), in the transitional regime the dependence of the drag force coefficient on the angular velocity is nonmonotonic. However, the variation of C_D over the range of W considered is relatively small and does not exceed 15%. The drag coefficient decreases with increase in W up to a certain limiting value W_* and after that starts to increase. An analysis of the stress distributions over the sphere surface shows that, on the whole, an increase in W results in an increase in the absolute value of the tangential stresses. The field of the normal stresses varies in a fairly complex manner. With increase in W, the contribution of the normal stresses ($C_D n$) decreases (see Table). At the same time, the contribution of the tangential stresses ($C_D \tau$) increases. For $\mathrm{W} < \mathrm{W}_*$ the value of $C_{D(n)}$ decreases faster than $C_{D(\tau)}$ increases. After that, $C_D(n)$ varies comparatively slowly, which results in an increase in the sum $C_D = C_{D(n)} + C_{D(\tau)}$.

From the viewpoint of the qualitative effect of the angular velocity coefficient on the Magnus force coefficient, for subsonic velocities, at $\mathrm{M} = 2$ the range of variation of W can be split into two intervals. For $\mathrm{W} < \mathrm{W}_{**} \sim 0.1$ the value of C_L decreases comparatively rapidly with increase in W. For $\mathrm{W} > \mathrm{W}_{**}$ the value of C_L also decreases but much more slowly. Thus, when W increases from 0.1 to 0.5, the value of C_L varies by not more than 4% of $|C_{L\infty}|$. This dependence of the Magnus force coefficient on the angular velocity is not consistent with either (3.2) or (3.3).

Due to the limitations of the numerical method used, we could not investigate in detail the behavior of $C_L(\mathrm{W})$ as $\mathrm{W} \to 0$. However, the calculation results show that in a subsonic flow, as W decreases for $\mathrm{W} \ll 1$, C_L increases mainly due to a significant increase in the contribution of the normal stresses $C_{L(n)}$, whereas the contribution of the tangential stresses $C_{L(\tau)}$ is small and varies only slightly.

In the case of supersonic flow, the variation of C_L on the range $0.03 \le \mathrm{W} \le 1$ turned out to be within the calculation error. However, for $\mathrm{W} > 1$ the Magnus force coefficient increases with W, which is the opposite of its behavior in a subsonic flow. This is attributable to the fact that, in a supersonic flow, as W increases, the absolute value of the contribution of the tangential stresses decreases, whereas in a subsonic flow it increases (see Table).

Despite the different form of the dependence $C_L(\mathrm{W})$ for sub- and supersonic flows, in both cases the fractions of the Magnus force $F_{L(\xi)}$ due to the normal and tangential stresses vary in a qualitatively similar manner. In the Table, the values of $C_{L(n)}$ and $C_{L(\tau)}$ were obtained by dividing the forces $F_{L(\xi)}$ by the scale F_L^*, which depends on W. The fractions of the Magnus force can be represented in the form $F_{L(\xi)} = C_L(\xi)\Omega F_L^{**}$, where the scale $F_L^{**} = p_\infty \pi R^2 S^2$ no longer depends on W. With increase in W, the absolute values of $C_{L(n)}\Omega$ and $C_{L(\tau)}\Omega$ always increase in absolute magnitude (see Table); however, this increase proceeds at different rates for sub- and supersonic flows, which results in a different form of the dependence $C_L(\mathrm{W})$.

10. TORQUE COEFFICIENT OF A SPINNING SPHERE

The calculated values of the torque coefficient C_T are presented in Fig. 7 as functions of $\mathrm{Re}_\omega = 16/(5\sqrt{\pi})\mathrm{W}/\mathrm{Kn}$ constructed for constant M and W.

In the transitional regime, for $\mathrm{Re}_\omega < 10$ and $\mathrm{W} = 0.1$ and for $\mathrm{Re}_\omega < 10^2$ and $\mathrm{W} = 1$ the torque coefficient C_T depends significantly on M, except in the case $\mathrm{M} \le 0.2$. At the same time, with increase in Re_ω the calculation results for C_T approach curve *8* obtained using (3.4) for the incompressible continuum flows in the absence of translational motion of the sphere relative to the gas, and the influence of the Mach number decreases. The nature of the curves in Fig. 7 makes it possible to assume that, at large Re_ω, the effect of the Mach number on the torque coefficient C_T is fairly small over the entire range of M considered. Accordingly, for $\mathrm{Re}_\omega > 10^2$–$10^3$ approximation (3.4) can also be used for compressible flows, at least as a first approximation.

Summary. A three-dimensional rarefied gas flow past a spinning sphere in the free-molecular and transitional flow regimes is studied using a direct statistical simulation method. A comparison of the calculated aerodynamic coefficients with the known data for the free-molecular and continuum flow regimes showed

that the compressibility and rarefaction effects make a significant impact on the Magnus force and the aerodynamic torque. The calculated values of the drag force coefficient for the transitional regime agree with the data of other authors. The dependences of all the aerodynamic coefficients on the angle between the translational and angular velocity vectors can be approximated with high accuracy by very simple trigonometrical functions. The maximum value of the aerodynamic-force component perpendicular to the drag force and the Magnus force does not exceed 10% of the maximum value of the latter, and the aerodynamic-torque component perpendicular to the translational and angular velocity vectors of the sphere almost vanishes. The direction of the Magnus force in the transitional regime is determined by the balance between the normal and tangential stresses on the sphere surface, whose contributions to the coefficient of this force are opposite in sign. The direction of this force changes at a certain critical Knudsen number, decreasing with increase in M. In the general case, the dependence of the Magnus force coefficient on the Reynolds number with transition from the free-molecular to the continuum flow regime is nonmonotonic. However, for Knudsen numbers greater than 0.05 the values of this coefficient vary monotonically and can be approximated by a fairly simple formula. In the transitional flow regime, the torque coefficient depends significantly on the Mach number. At the same time, with increase in the Reynolds number based on the angular velocity this dependence becomes weaker.

REFERENCES

1. S.I. Rubinow and J.B. Keller, "The Transverse Force on a Spinning Sphere Moving in a Viscous Fluid," J. Fluid Mech. **11** Pt 3, 447–459 (1961).
2. S.A. Morsi and A.J. Alexander, "An Investigation of Particle Trajectories in Two-Phase Flow Systems," J. Fluid Mech. **55** Pt 2, 193–208 (1972).
3. N.A. Zarin, *Measurement of Non-Continuum and Turbulence Effects on Subsonic Sphere Drag* (NASA Report NCR-1585, 1970).
4. W.R. Lawrence, *Free-Flight Range Measurements of Sphere Drag at Low Reynolds Numbers and Low Mach Numbers* (Arnold Eng. Development Center. Report AEDC-TR-67-218, 1967).
5. A.B. Bailey and J. Hiatt, *Free-Flight Measurements of Sphere Drag at Subsonic, Transonic, Supersonic, and Hypersonic Speeds for Continuum, Transition, and Near-Free-Molecular Flow Conditions* (Arnold Eng. Development Center. Report AEDC-TR-70-291, 1971).
6. A.B. Bailey and J. Hiatt, "Sphere Drag Coefficients for a Broad Range of Mach and Reynolds Numbers," AIAA J. **10** (11), 1436–1440 (1972).
7. C.B. Henderson, "Drag Coefficients of Spheres in Continuum and Rarefied Flows," AIAA J. **14** (6), 707–708 (1976).
8. L.E. Sternin, B.N. Maslov, A.A. Shraiber, and A.M. Podvysotskii, *Two-Phase Mono- and Polydisperse Gas-Particle Flows* [in Russian] (Mashinostroenie, Moscow, 1980).
9. P.P. Brown and D.F. Lawler, "Sphere Drag and Settling Velocity Revisited," J. Environment. Eng. **129** (3), 222–231 (2003).
10. Ch.-T. Wang, "Free-Molecular Flow over a Rotating Sphere," AIAA J. **10** (5), 713–714 (1972).
11. S.G. Ivanov and A.M. Yashin, "Forces and Moments Acting on Bodies Rotating about a Symmetry Axis in Free Molecular Flow," Fluid Dynamics **15** (3), 449 (1980).
12. H. Niazmand and M. Renksizbulut, "Surface Effects on Transient Three-Dimensional Flows Around Rotating Spheres at Moderate Reynolds Numbers," Computers and Fluids **32** (10), 1405–1433 (2003).
13. Y. Tsuji, Y. Morikawa, and O. Mizuno, "Experimental Measurements of the Magnus Force on a Rotating Sphere at Low Reynolds Numbers," Trans. ASME. J. Fluids Eng. **107** (4), 484–488 (1985).
14. B. Oesterle and T. Bui Dinh, "Experiments on the Lift of a Spinning Sphere in a Range of Intermediate Reynolds Numbers," Experim. Fluids **25** (1), 16–22 (1998).
15. J.H. Maccoll, "Aerodynamics of a Spinning Sphere," J. Roy. Aeronaut. Soc. **32** 777–798 (1928).
16. V.A. Naumov, A.D. Solomenko, and V.P. Yatsenko, "Effect of the Magnus Force on the Motion of a Rigid Spherical Body at a High Angular Velocity," Inzh. Fiz. Zh. **65** (3), 287–290 (1993).
17. N. Chegroun and B. Oesterle, "Etude Numérique de la Trainée, de la Portance et du Couple sur une Sphere en Translation et en Rotation," (Actes 11éme Congrés Francais Mecanique, Lille-Villeneuve d'Ascq, France, 1993. V. 3), 81–84.

18. S.C.R. Dennis, S.N. Singh, and D.B. Ingham, "The Steady Flow due to a Rotating Sphere at Low and Moderate Reynolds Numbers," J. Fluid Mech. **101** Pt 2, 257–279 (1980).
19. K.I. Borg, L.H. Soderholm, and H. Essen, "Force on a Spinning Sphere Moving in a Rarefied Gas," Phys. Fluids **15** (3), 736–741 (2003).
20. P.D. Weidman and A. Herczynski, "On the Inverse Magnus Effect in Free-Molecular Flow," Phys. Fluids. **16** (2), L9–L12 (2004).
21. A.N. Volkov, "Numerical Modeling of the Magnus Force and the Aerodynamic Torque on a Spinning Sphere in Transitional Flow," (Proc. 25th Int. Symp. Rarefied Gas Dynamics, St. Petersburg, Russia, 2006) (Eds. M. Ivanov and A. Rebrov, SBRAS Press, Novosibirsk, 2007), 771–776.
22. M.N. Kogan, *Rarefied-Gas Dynamics* [in Russian] (Nauka, Moscow, 1967).
23. G.A. Bird, *Molecular Gas Dynamics and the Direct Simulation of Gas Flows* (Clarendon Press, Oxford, 1994).
24. F.C. Hurlbut, "On the Molecular Interactions between Gases and Solids," in: *Dynamics of Manned Lifting Planetary Entry* (Wiley, New York, 1963), 754–777.
25. V.P. Shidlovskii, *Introduction to Rarefied Gas Dynamics* [in Russian] (Nauka, Moscow, 1965).
26. G. Kirchhoff, *Vorlesungen* ü*ber Mathematische Physik: Mechanik* (Teubner, Leipzig, 1876).
27. O.M. Belotserkovskii, A.I. Erofeev, and V.E. Yanitskii, "Nonstationary Method of Direct Statistical Simulation of Rarefied Gas Flows," Zh. Vych. Matem. Mat. Fiz. **20** (5), 1174–1204 (1980).
28. M.S. Ivanov and S.V. Rogazinskii, "Comparative Analysis of the Algorithms of the Direct Statistical Simulation Method in Rarefied Gas Dynamics," Zh. Vych. Matem. Mat. Fiz. **28** (7), 1058–1070 (1988).
29. A.N. Volkov, "The Aerodynamic and Heat Properties of a Spinning Spherical Particle in Transitional Flow," (Proc. 6th Int. Conf. Multiphase Flow, Leipzig, ICMF'2007, CD, Paper S2 Mon_C_6).
30. V.V. Riabov, "Aerodynamics of a Spinning Cylinder in Rarefied Gas Flows," J. Spacecraft and Rockets **36** (3), 486–488 (1999).